Irreversibility lines in the ***H***- ***T*** phase diagram of re-entrant amorphous ferromagnets

1998 J. Phys.: Condens. Matter 10 11067

(http://iopscience.iop.org/0953-8984/10/48/026)

J. Phys.: Condens. Matter **10** (1998) 11067–11080. Printed in the UK PII: S0953-8984(98)96406-2

Irreversibility lines in the H–T phase diagram of re-entrant amorphous ferromagnets

S N Kaul† and S Srinath

School of Physics, University of Hyderabad, Central University PO, Hyderabad 500 046, Andhra Pradesh, India

Received 31 July 1998

Abstract. The longitudinal components of the 'zero-field-cooled' (M_{ZFC}) and 'field-cooled' (M_{FC}) magnetization of amorphous $Fe_{90-x}TM_xZr_{10}$ (TM = Co, Ni) and $Fe_{90+y}Zr_{10-y}$ re-entrant ferromagnetic alloys have been measured in the static mode and at different thermal cycling rates varying from 0.01 K min^{-1} to 2 K min^{-1} in constant magnetic fields (H) ranging between 1.5 Oe and 15 kOe. The difference, $M_{irr}(T) = M_{FC}(T) - M_{ZFC}(T)$, is taken to be the direct measure of irreversibility in magnetization. The onset of weak irreversibility and a *crossover* from weak to strong irreversibility are observed at the temperatures $T_{GT}(H)$ and $T_{AT}(H)$, respectively, for fields $H < H^*$; H^* depends on x and y. $T_{GT}(H)$ and $T_{AT}(H)$ follow the relations $\{1 - [T_{GT}(H)/T_{GT}(0)]\} = A_{GT}h$ and $\{1 - [T_{AT}(H)/T_{AT}(0)]\}^3 = A_{AT}h^2$, where $h = g\mu_B H/k_B T^0$ (T^0 stands for $T_{GT}(0)$ or $T_{AT}(0)$), which have the same form as those predicted by the modified versions of the Gabay–Toulouse (GT) and de Almeida–Thouless (AT) mean-field (MF) theories that include non-vanishing spontaneous magnetization, but the observed values of the coefficients A_{GT} and A_{AT} are *several orders of magnitude larger* than the MF estimates. $T_{AT}(H)$ is relatively *insensitive* while $T_{GT}(H)$ is *extremely sensitive* to thermal cycling rates (TCR) if they exceed a threshold value. The physical implications of extremely large magnitudes of A_{GT} and A_{AT}, and of the observed TCR-induced shifts in the GT and AT irreversibility lines in the H–T plane, have been brought out clearly while discussing these results in terms of the existing theoretical models.

1. Introduction

The phenomenon called *re-entrance*, in which a substance re-enters a *disordered* phase at low temperatures after it had existed in an *ordered* (a disordered) phase at intermediate (high) temperatures, occurs in physical systems as disparate as binary liquid mixtures, magnets, superconductors and liquid crystals. In magnetic materials, re-entrance has been observed [1–3] regardless of whether they are crystalline or amorphous, insulating (localized-electron systems) or metallic (itinerant-electron systems), ferromagnetic or antiferromagnetic. Even though re-entrant behaviour is widespread in magnetic systems, several basic issues concerning the nature of the re-entrant (RE) state and the RE transition remain highly controversial, as elucidated below. Mean-field (MF) vector-spin models [4, 5] predict the following sequence of phase transitions as the temperature of the system is lowered:

(i) a phase transition from a paramagnetic (PM) to a ferromagnetic (FM) state at the Curie temperature T_C,

† Author to whom any correspondence should be addressed. E-mail: kaulsp@uohyd.ernet.in.

0953-8984/98/4811067+14$19.50

(ii) a transition from a FM to a 'mixed' M_1 state (in which *longitudinal* FM order *coexists* with *transverse* spin-glass (SG) order) at the Gabay–Toulouse (GT) phase boundary [5] and

(iii) a 'mixed' $M_1 \rightarrow$ 'mixed' M_2 phase transition along the de Almeida–Thouless (AT) instability line [4, 5] that signals a *crossover* from weak to strong irreversibility.

Traditionally, the transition to the RE state is characterized by a sharp drop in the real part of the ('zero-field') ac susceptibility (χ'_{ac}) and 'zero-field-cooled' (ZFC) magnetization, M_{ZFC}, from their demagnetizing-factor-limited values for temperatures below the re-entrant transition temperature T_{RE}. However, scientific opinion on the interpretation of this attribute of the RE transition is divided. On the one hand, the drop in $\chi'_{ac}(T)$ and $M_{ZFC}(T)$ for $T < T_{RE}$ is taken to indicate a complete destruction [6–9] of long-range ferromagnetic order and a transition to the SG state. On the other hand, it is argued that this experimental result, far from representing a transition to a SG state, is merely a consequence of the exponentially increasing [10, 11] coercivity and the concomitant magnetic hardness of the ferromagnetic system on cooling through T_{RE}. Similarly, a sudden *appearance* [12–15] of the second and fifth lines of the sextet (corresponding to $\Delta m_I = 0$ transitions) in Mössbauer spectra measured at $T \leqslant T_{RE}$ in external magnetic fields (applied *along* the γ-ray direction and *strong enough* to *saturate* the magnetic specimen) is regarded as direct experimental evidence for the freezing of transverse spin components (i.e., for the GT transition) but such experiments fail to resolve the issue of whether the ferromagnetic ordering of the longitudinal spin components is '*spontaneous*' or '*field induced*'. From the foregoing remarks, it is evident that (a) no rigorous correlation [16, 17] has so far been established between the MF model phase boundaries and the structure usually observed in thermomagnetic curves and (b) no experimental test is currently available to unambiguously ascertain whether or not the re-entrant transition is cooperative in nature.

Now that the mean-field theories [5, 18] predict that the reduced GT transition temperature $\tau_{GT}(H) = 1 - T_{GT}(H)/T_{GT}(0)$, at *low* fields, varies with external magnetic field (H) as H^2 for a *pure* spin glass and as H for a spin system with *longitudinal* ferromagnetic order (spontaneous magnetization) and *transverse* spin-glass order (for details, see section 2), a detailed study of the field dependence of T_{GT} should provide an unambiguous way of distinguishing between a pure spin-glass state and a *mixed* state in which the longitudinal spin components are ferromagnetically ordered while the transverse spin components exhibit spin-glass order. Bulk magnetization, $M(H, T)$, and initial-susceptibility measurements [19–22], performed, in the past, on a wide variety of spin-glass systems to determine the field dependences of the PM–SG, AT and GT transition temperatures (i.e., T_{SG}, T_{AT} and T_{GT}, respectively), have yielded a great deal of useful information about the nature of the phase transitions occurring at T_{SG}, T_{AT} and T_{GT}. By comparison, such studies on re-entrant systems are extremely rare [18, 23]. Dubiel *et al* [18] have determined $\tau_{GT}(H)$ from 'in-field' Mössbauer measurements on re-entrant $Cr_{75}Fe_{25}$ alloy and found a *linear* variation of τ_{GT} with H for $H > 10$ kOe. This observation is, however, not consistent with the prediction of the MF theory [18] that such a relationship between τ_{GT} and H should hold at *low* fields only. By contrast, Kunkel *et al* [23] observe that the 'high-temperature' peak position (T_p) in the imaginary component of the complex susceptibility varies linearly with H for $H \leqslant 40$ Oe for re-entrant $Ni_{77.5}Mn_{22.5}$ alloy, but no rigorous connection between T_p and T_{GT} could be established. Furthermore, going by the wealth of information already gathered for the case of spin glasses [19, 21, 22], investigation of the time-dependent effects associated with GT and AT lines in the H–T phase diagrams of re-entrant spin systems is expected to provide decisive experimental evidence for or against cooperative nature of the phase transitions at T_{GT} and T_{AT}. Recognizing the merits of the studies that bring out clearly

the field dependences and dynamic aspects of GT and AT lines for re-entrant systems, we have performed extensive bulk magnetization measurements on re-entrant $Fe_{90-x}TM_xZr_{10}$ (TM = Co, Ni) and $Fe_{90+y}Zr_{10-y}$ amorphous alloys. In order to facilitate discussion of the results in terms of the existing theories, we give a brief account of the theoretical models, proposed in the literature for re-entrant spin systems, in the following section.

2. Theoretical models: a brief résumé

Sherrington–Kirkpatrick (SK) mean-field (MF) theory [24] and its extensions [4, 5] deal with spin systems in which each spin interacts with all of the remaining spins through an (infinite-ranged) exchange interaction which has a Gaussian distribution, centred at J_0, with standard deviation J. For $J_0 = 0$ (i.e., when exchange interactions are *random* in *sign* and frustration leads to spin-glass order), these theories predict *finite-temperature* phase transition in *zero* as well as *finite* magnetic fields for both Ising and Heisenberg spin-glass (SG) systems. In an Ising SG system, this transition in the field–temperature (H–T) phase diagram occurs along the de Almeida–Thouless (AT) line [4]:

$$\tau_f^3(h) = (3/4)h^2 \tag{1}$$

where $\tau_f(h) = 1 - T_f(H)/T_f(0)$, $h = g\mu_B H/k_B T_f(0)$ is *small* and $T_f(0)$ is the SG freezing temperature for $H = 0$. In an *isotropic* spin-glass system composed of vector spins with n components, transitions in the H–T plane occur at *low* fields along two phase transition lines [5]: the Gabay–Toulouse (GT) line [5]:

$$\tau_{GT}(h) = 1 - T_{GT}(H)/T_f(0) = Ch^2 \tag{2}$$

with $C = (n^2 + 4n + 2)/4(n + 2)^2$, which marks the freezing of spin degrees of freedom *transverse* to the field direction and the onset of *weak* irreversibility, is followed at lower temperatures by another line [4, 5]:

$$\tau_{AT}^3(h) = [1 - T_{AT}(H)/T_f(0)]^3 = C'h^2 \tag{3}$$

with $C' = (n + 1)(n + 2)/8$, which reduces to the AT line, equation (1), for $n = 1$ and signals the freezing of spin degrees of freedom *along* the field direction as well as a *crossover* from *weak* to *strong* irreversibility.

Kotliar and Sompolinsky [25] (KS) were the first to recognize that the random anisotropy (caused by anisotropic Dzyaloshinsky–Moriya interactions), invariably present in real spin-glass systems, can significantly alter both the form and nature of the finite-field transition, even when average anisotropy constant $D \ll J$ and hence has practically no effect on the zero-field transition. In the range $h^{2/3} \ll d$ $(=D/k_BT)$, termed by KS the *strong-anisotropy regime*, the transition is of the AT type, in that the transition line is described by equation (3) but with C' replaced by another constant, $C'' = (n + 2)/4n$. In this region, random anisotropy causes a strong mixing of the longitudinal and transverse spin components. In the *weak-anisotropy limit*, $d \ll h^{5/2}$, the transition is identical to the GT one, equation (2), but the zero-field transition temperature, $T_f(0)$, shifts to lower temperatures by an amount which depends on the magnitude of d in accordance with the relation [26]

$$\tilde{T}_f(0) = T_f(0) - [(n + 2)/2(n + 1)^{1/2}]d.$$

Moreover, the *transverse* Edwards–Anderson order parameter [27] ($q_T \propto d$) possesses a *finite* [26] value on this critical line, so the freezing of transverse spin components occurs above this line in the H–T phase diagram, where $q_T = 0$.

As far as the finite-temperature transitions in zero and finite magnetic fields in re-entrant spin systems with J_0 *positive* and $J_0 > J$ are concerned, the mean-field theories [4, 5, 18]

make the following predictions. If the spin system is cooled in *zero* field, the Gabay–Toulouse model [5] predicts the sequence of phase transitions as PM $\rightarrow$ FM $\rightarrow$ 'mixed' phase M_1 $\rightarrow$ 'mixed' phase M_2. In the ferromagnetic (FM) state, long-range FM order in the longitudinal direction, henceforth referred to as collinear ferromagnetism, coexists with randomly oriented but otherwise free transverse spin components which average out to zero at any instant of time. The mixed M_1 phase consists of both collinear ferromagnetism (i.e., spontaneous magnetization) and transverse spin components which *cooperatively* freeze in random orientations at the transition temperature $T_{FM\rightarrow M_1} = T_{GT}(H = 0)$ that marks the onset of *weak* irreversibility in magnetization. M_2 is a mixed phase in which *longitudinal* FM order coexists with *transverse* spin-glass order, as in M_1, but the transition to this phase is marked by the spontaneous replica-symmetry breaking of the SK solution, similar to that observed previously by de Almeida and Thouless for the Ising case and interpreted as a crossover from weak to strong irreversibility in magnetization. By contrast, the effect of *finite* external magnetic field (H) on the AT and GT critical lines in the H–T phase diagram of a spin system with *positive* J_0 and $J_0 \gtrsim J$ is to leave the functional dependence of τ_{AT} on h, i.e., equation (3), *unaltered* but *change* the field dependence of T_{GT} from $\tau_{GT}(h) \sim h^2$, equation (2), in the case of a spin-glass system with $J_0 = 0$, to [18]

$$\tau_{GT}(h) = 1 - T_{GT}(H)/T_{GT}(0) = (2^{3/2}C)h \tag{4}$$

where $T_{GT}(0) \equiv T_{GT}(H = 0)$ is the GT transition temperature in the absence of external magnetic field and equation (4) is *valid* for $H \ll M_S$ (spontaneous magnetization).

Non-mean-field models for re-entrant ferromagnetic systems include the phenomenological models, proposed independently by Coles *et al* [28] and Kaul [29] (K), that visualize such systems, in the ferromagnetic state, to be composed of an *infinite* three-dimensional (3D) FM cluster (matrix) and *finite* spin clusters (consisting of a set of ferromagnetically coupled spins). Though these models are apparently similar, their underlying mechanisms are completely different in that the spatial segregation of finite spin clusters and the FM matrix in the model of Coles *et al* [28] is due to fluctuation in composition at the microscopic scale whereas in the K-model [29] it arises from *local (atomic) density* fluctuations [30, 31]. While the former model is more appropriate for crystalline re-entrant systems than for amorphous re-entrant systems, the reverse is true for the latter model. According to these models, the freezing of finite spin clusters of widely different size is a *thermally activated process* [2, 32] and occurs over a wide range of temperatures such that at low temperatures, a 'mixed' state (in which the ferromagnetic order of the matrix coexists with the finite clusters frozen in random orientations, i.e., with cluster spin-glass order) forms the ground state of the system. Therefore, unlike mean-field models, such phenomenological models predict that the transition from a FM to a mixed state is *not a true thermodynamic phase transition.*

3. Experimental details

Amorphous (a-) $Fe_{90-x}TM_xZr_{10}$ (TM = Co, Ni and $x = 0$, 1, 2, 4, 6) and $Fe_{90+y}Zr_{10-y}$ ($y = 0.0$, 0.5) alloys were prepared and characterized by methods described in detail in our previous reports [31, 33, 34]. Several strips of the alloy ribbon, all of 3 mm length and 1–2 mm width, were stacked one above another after giving them a thin coat of Apeizon N grease. This arrangement ensured good thermal contact between the ribbon strips. The sample in the form of a stacked bundle was placed in the sample holder assembly and rotated such that the external magnetic field (H) lies along the length in the ribbon plane. Such a sample orientation minimizes the demagnetizing effects. Sample temperature was

monitored by pre-calibrated carbon-glass ($T \leqslant 40$ K) and platinum ($T > 40$ K) sensors which were in body contact with the sample. *Zero-field-cooled*, $M_{ZFC}(T)$, and *field-cooled*, $M_{FC}(T)$, magnetizations of the alloy samples as functions of temperature at *fixed* values of H ranging between 1.5 Oe and 15 kOe were measured on an EG&G Princeton Applied Research 4500 Vibrating Sample Magnetometer (VSM) using the following procedure. To measure $M_{ZFC}(T)$, the sample was cooled down to the lowest temperature, 3.8 K, in *zero field*; after a waiting time of 30 min, the field was switched on and held constant (to within ± 0.05 Oe) at a specific value (say H^*) and static magnetization was measured as the sample was heated to a temperature T^* which lies well above the Curie point, T_C. When the sample temperature reached T^*, the sample was cooled down to 3.8 K in the *same* field H^* and magnetization measured as a function of temperature to obtain $M_{FC}(T)$. In order to investigate the time-dependent effects associated with $M_{ZFC}(T)$ and $M_{FC}(T)$, the sample was subjected to two different (*static* and *dynamic*) thermal cycling treatments. In the *static* mode, sample temperature was held constant (to within ± 5 mK) at a certain value in the range 3.8 K $\leqslant T \leqslant T^*$ and after a waiting time of 20 min, magnetization was measured; this scheme was followed to measure M_{ZFC} and M_{FC} at *fixed* temperatures 0.1 K (0.5 K) apart in the range 3.8 K $\leqslant T \leqslant 50$ K ($50 < T \leqslant T^*$) during heating and cooling runs, respectively. In the *dynamic* mode, $M_{ZFC}(T)$ and $M_{FC}(T)$ were measured while maintaining the heating and cooling rates constant at a value that ranges between 0.01 K min^{-1} and 2 K min^{-1}.

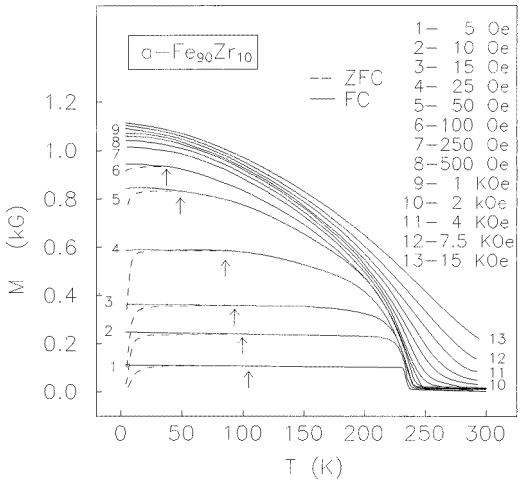

Figure 1. Temperature variations of the 'zero-field-cooled' (ZFC) and 'field-cooled' (FC) magnetizations at different but fixed values of the external magnetic field for amorphous $Fe_{90}Zr_{10}$. The $M_{ZFC}(T)$ and $M_{FC}(T)$ data shown in this figure were taken at a constant thermal cycling rate of 2 K min^{-1}. The bifurcation temperatures $T_1(H)$ (see the text) are indicated by upward-pointing arrows.

4. Results and discussion

Figures 1 and 2 depict the temperature variations of M_{ZFC} and M_{FC} at a few selected values of the external magnetic field under two extreme conditions, i.e., when the heating and cooling rates were maintained constant at 2 K min^{-1} (figure 1) and when the *static* mode

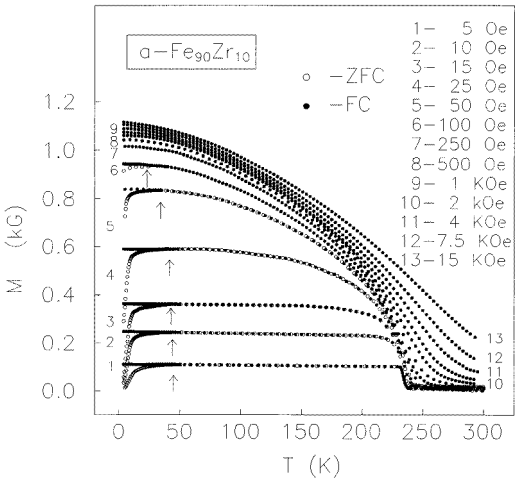

Figure 2. 'Zero-field-cooled' (ZFC) and 'field-cooled' (FC) magnetizations of amorphous $Fe_{90}Zr_{10}$ as functions of temperature at different but fixed values of the external magnetic field. These data were taken in the static mode (see the text). Only one-fifth of the total number of data points are shown in this figure for the sake of clarity. Upward-pointing arrows indicate the bifurcation temperatures $T_1(H)$ (see the text).

of measurement (mentioned in section 3) was employed (figure 2). The data presented in figures 1 and 2 capture all of the essential features of similar thermomagnetic curves obtained for other compositions investigated in this work. The main features of the $M_{ZFC}(T)$ and $M_{FC}(T)$ curves for different compositions obtained in both static and dynamic modes of measurement are listed below.

(i) For fields below a certain value, which decreases (increases) with increasing TM (Fe) concentration in $Fe_{90-x}TM_xZr_{10}$ ($Fe_{90+y}Zr_{10-y}$) alloys, $M_{ZFC}(T)$ and $M_{FC}(T)$ curves *bifurcate* at a temperature T_1 and $M_{ZFC}(T)$ exhibits a 'knee' at a temperature T_2 in the low-temperature region; both T_1 and T_2 are *field dependent*.

(ii) Irrespective of the value of H, $M_{ZFC}(T)$ and $M_{FC}(T)$ data taken either in the *static* mode or with thermal cycling rates (TCR) $\lesssim 0.02$ K min^{-1} are *reproducible* (within the resolution limit of 5×10^{-5} emu of the VSM) and so are the temperatures $T_1(H)$ and $T_2(H)$.

(iii) While $M_{FC}(T)$ is not significantly altered, $M_{ZFC}(T)$ is *extremely sensitive* to the TCR in the range 0.05 K min^{-1} $\lesssim$ TCR $\lesssim$ 2 K min^{-1}—so much so that M_{ZFC} coincides with M_{FC} at a temperature which shifts to higher temperatures as TCR increases in the above range. Consequently, with increasing TCR, $T_1(H)$ assumes *higher* values whereas $T_2(H)$ gets displaced to higher temperatures by a very small amount or even remains *essentially unaltered* such that the functional dependences of both T_1 and T_2 on H do not change significantly. This fact is borne out clearly by the *representative* data presented in figures 1 and 2 in that $T_1(H)$ for $H \leqslant 10$ Oe determined at TCR $= 2$ K min^{-1} is $\sim$2.5 *times larger* in magnitude than $T_1(H \leqslant 10$ Oe) deduced from static measurements whereas $T_2(H)$ is nearly the same in the two cases; moreover, the difference between the corresponding values of T_1 goes on reducing rapidly as H increases. It should, however, be noted that the scatter in the $T_1(H)$ and $T_2(H)$ data increases with increasing TCR.

Considering the above observations (ii) and (iii), we first focus our attention on the results of static measurements, and discuss the dynamic aspects of $M_{ZFC}(T)$ and $M_{FC}(T)$ at a

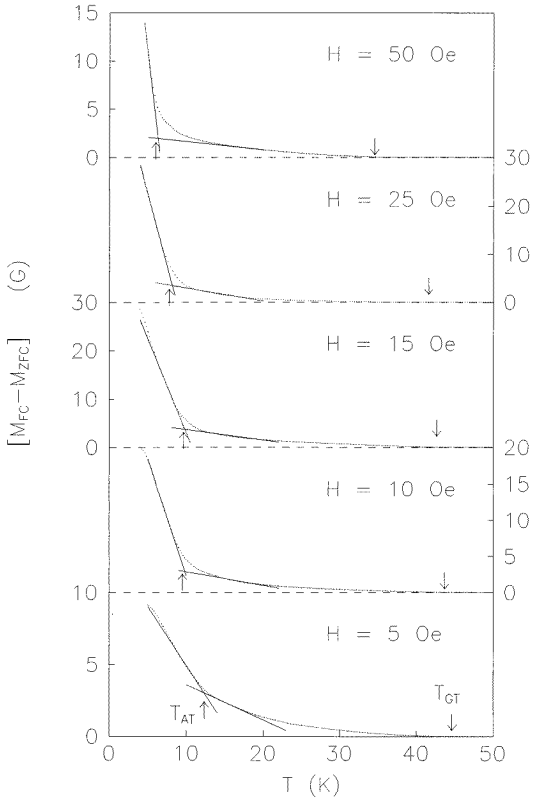

Figure 3. The difference $M_{\rm irr} = M_{\rm FC} - M_{\rm ZFC}$ at different but fixed values of H plotted against temperature. This figure serves to illustrate the method used by us to determine the temperatures $T_{\rm GT}$ and $T_{\rm AT}$.

later stage.

Obviously, the difference between the values of $M_{\rm FC}$ and $M_{\rm ZFC}$ at a given temperature is a *direct measure* of the irreversibility in magnetization at that temperature, i.e., $M_{\rm irr}(T) = M_{\rm FC}(T) - M_{\rm ZFC}(T)$. Figure 3 displays *representative* $M_{\rm irr}(T)$ curves at a few selected but fixed values of H, constructed out of the $M_{\rm FC}(T)$ and $M_{\rm ZFC}(T)$ data taken at such fields using the static mode of measurement (cf. figures 2 and 3). The temperature that marks the onset of *weak* irreversibility in magnetization, i.e., $T_{\rm GT}(H)$, is determined from these curves as the temperature at which $M_{\rm irr}(T)$ begins to depart from *zero*. The temperatures $T_{\rm GT}(H)$ ($=T_1(H)$, the bifurcation temperature defined above) are indicated by downward-pointing arrows in figure 3. By the same token, a crossover from weak to strong irreversibility in magnetization manifests itself in an *upturn* in the $M_{\rm irr}(T)$ curve below a certain temperature as T is lowered below $T_{\rm GT}$. We estimate the values of $T_{\rm AT}$ at different fields by the method illustrated in figure 3. The values of $T_{\rm AT}(H)$ ($\cong T_2(H)$, the 'knee' temperature defined above) so obtained are indicated in this figure by upward-pointing arrows. It is immediately noticed that both $T_{\rm GT}$ and $T_{\rm AT}$ *shift* to *lower* temperatures as the magnitude of H *increases*. With the values of $T_{\rm GT}$ and $T_{\rm AT}$ at different values of H determined, the next step is to verify the theoretical predictions of equations (2)–(4). To this end, the expressions $T_{\rm GT}(H) = T_{\rm GT}(0)[1 - AH^p]$ and $T_{\rm AT}(H) = T_{\rm AT}(0)[1 - A'H^q]$ have been least-squares-fitted to the $T_{\rm GT}(H)$ and $T_{\rm AT}(H)$ data with the result that these expressions with $p = 1.00(2)$ and $q = 0.66(2)$ reproduce the observed variations quite well for $H \lesssim 40$ Oe but fail to do so at higher fields (note that the deviations of the data from the best least-squares (LS) fits based on the above expressions could be discerned only in those cases, i.e., with $x \leqslant 4$ for

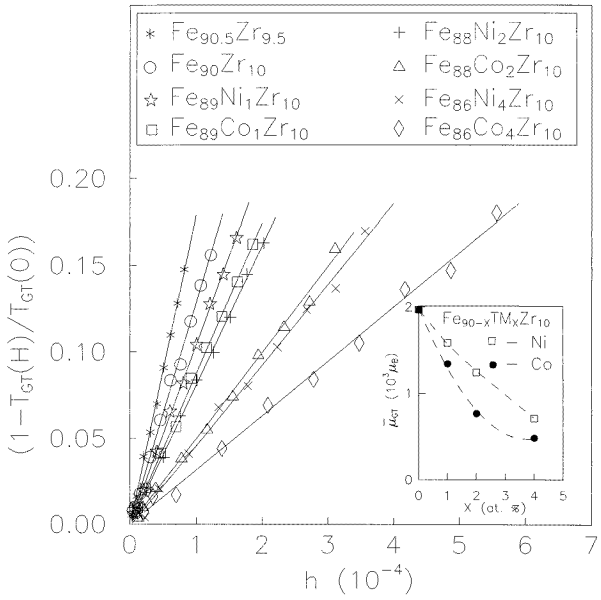

Figure 4. $[1 - T_{GT}(H)/T_{GT}(0)]$ versus h plots for the amorphous alloys investigated. The straight lines through the data points represent the best least-squares fits based on equation (4) of the text. The inset shows the average magnetic moment $\bar{\mu}_{GT}$ participating in the GT 'transition' plotted against the TM (=Co, Ni) concentration. The dashed curves through $\bar{\mu}_{GT}(x)$ data points serve as a guide to the eye.

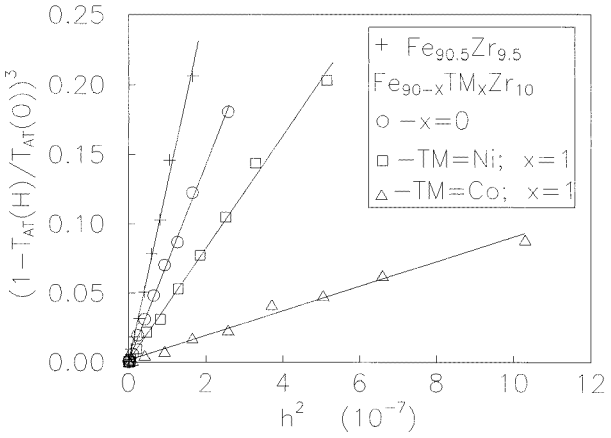

Figure 5. $[1 - T_{AT}(H)/T_{AT}(0)]^3$ versus h^2 plots for different alloy compositions. The straight lines through the data points denote the best least-squares fits based on equation (3) of the text.

$T_{GT}(H)$ and $x \leqslant 1$ for $T_{AT}(H)$, for which $T_{GT}(H)$ and $T_{AT}(H)$ could be determined even for $H \gtrsim 50$ Oe). Using the values of $T_{GT}(0)$ and $T_{AT}(0)$ obtained from such LS fits for the alloys with $x \leqslant 4$, $y \leqslant 0.5$, respectively, as well as those of the Landé splitting factor g estimated for the same compositions previously from ferromagnetic resonance (FMR) data [33], $\tau_{GT}(h)$ versus h and $\tau_{AT}^3(h)$ versus h^2 plots are constructed from the raw $T_{GT}(H)$

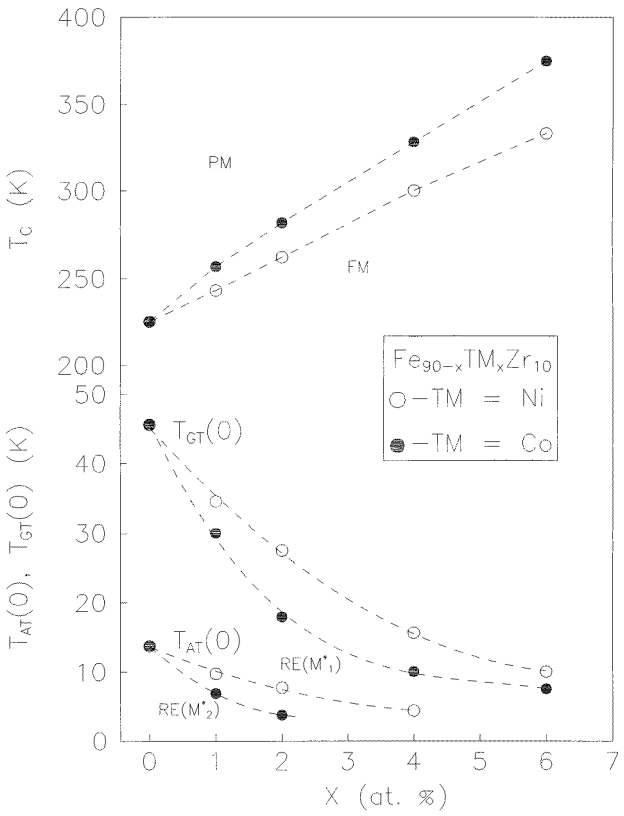

Figure 6. The 'zero-field' magnetic 'phase diagram' for amorphous $Fe_{90-x}TM_xZr_{10}$ (TM = Co, Ni) alloys. The abbreviations PM, FM, RE(M^*_1) and RE(M^*_2) stand for the paramagnetic, ferromagnetic, re-entrant (mixed phase 1) and re-entrant (mixed phase 2) phases, respectively.

and $T_{AT}(H)$ data and displayed in figures 4 and 5. The variations of $T_{GT}(0)$ and $T_{AT}(0)$ with the TM concentration x together with the x-dependence [34] of T_C (determined by the 'kink-point' method [34]) are depicted in figure 6. Note that the numerical estimates of $T_{GT}(0)$ and $T_{AT}(0)$ for the compositions $x = 6$ and $x = 2$, 4, respectively, shown in figure 6, are actually the values determined at the lowest field $H = 1.5$ Oe, because for these compositions T_{GT}, $T_{AT} < 10$ K and the field range over which the field dependences of T_{GT} and T_{AT} could be monitored is extremely narrow. At this stage, it should be emphasized that both $T_{GT}(0)$ and $T_{AT}(0)$ (the latter to a lesser extent) are *time-dependent* and the values of these quantities displayed in figure 6 are obtained in the so-called 'long-observation-time limit'. In this limit, the irreversibility lines of GT and AT type (and hence $T_{GT}(0)$ and $T_{AT}(0)$) are apparently time independent.

The salient features of the data presented in figures 4 and 5 are: (I) the $T_{GT}(H)$ data are *better* described [35] by equation (4) than by equation (2); and (II) the observed values (A_{AT} and A_{GT}) of the coefficients (C' and $2^{3/2}C$) of the h^2- and h-terms in equations (3) and (4) are *several orders of magnitude larger* than those theoretically predicted [5, 18] for a spin system with $n = 3$. In view of the theoretical considerations leading to equations (2) and (4) (section 2), our observation (I) unambiguously demonstrates that the re-entrant state in the systems investigated here is *not* a pure spin-glass state but a *mixed* state in which *long-*

range ferromagnetic order (finite spontaneous magnetization, M_S) coexists with spin-glass order. Moreover, considering that the definition of the reduced field, i.e., $h = g\mu_B H/k_B T^0$ (where $T^0 = T_{AT}(0)$ or $T_{GT}(0)$), in equations (3) and (4) is based on the assumption that the so-called AT and GT 'transitions' involve an elementary moment of *one* μ_B, the coefficients A_{AT} and A_{GT} can possess unusually large values only when the average moment (in units of μ_B) participating in such 'transitions' is several orders of magnitude *larger*. Thus, *extremely large* magnitudes of the proportionality constants in equations (3) and (4) indicate that the *average* elementary moments participating in AT and GT 'transitions', far from being the moments of individual spins as envisaged in the mean-field models [4, 5, 18], are those of *giant (finite) spin clusters* (groups of ferromagnetically coupled spins). This interpretation permits a reasonably accurate determination of the *average* moment ($\bar{\mu}_{GT}$) of the clusters taking part in the GT 'transition' in that $\bar{\mu}_{GT}$ is nothing but the *ratio* of the *observed* value (A_{GT}) of the *slope* of the $\tau_{GT}(h)$ versus h straight line (figure 4) to 0.6505 (=the theoretical value [5, 18] of $2^{3/2}C$ for a spin system with $n = 3$). The values of $\bar{\mu}_{GT}$ for different x, so computed, are plotted against the TM concentration x in the inset of figure 4. However, the numerical estimates of the *average* moments of clusters involved in the AT 'transition' $\bar{\mu}_{AT}$ arrived at in the same way, i.e., $\bar{\mu}_{AT} = A_{AT}/C'$, turn out to be *two* to *four* times *smaller* than $\bar{\mu}_{GT}$, depending on the alloy composition. The existence of finite spin clusters with average moments as large as estimated in this work has also been *previously* inferred from bulk magnetization [30, 31, 36], Mössbauer [3, 14, 32, 37, 38], FMR [3, 33], electrical noise [39] and small-angle neutron scattering [40, 41] measurements on amorphous alloys with the same (or similar) nominal composition as those used in the present investigation. Furthermore, persistence of long-range ferromagnetic order (and hence of *finite* M_S) down to the lowest temperature, which lies well below $T_{GT}(0)$ (the re-entrant transition temperature), in the glassy alloys in question is also firmly supported by the results of earlier magnetization [30, 31, 35], Mössbauer [3, 14, 15, 32, 38], FMR [3, 33], Lorentz electron microscopy [42], Kerr-effect [43], neutron depolarization [44] and inelastic neutron scattering [45] experiments. Foregoing arguments, therefore, permit us to conclude that, consistent with the predictions of the K-model [29–33], the re-entrant state in the amorphous spin systems investigated is a *mixed* state in which *long-range* ferromagnetic order (i.e., an *infinite* 3D FM matrix) *coexists* with *cluster* spin-glass order (i.e., *finite* spin clusters frozen in random orientations).

Having discussed the results of the measurements taken in the *static* mode, we now focus our attention on the aforementioned observation (iii), i.e., on the *time-dependent shifts* in $T_{GT}(H) \equiv T_1(H)$ and $T_{AT}(H) \equiv T_2(H)$. Considering that the mean-field (MF) theories [4, 5, 18] assert that the GT and AT transitions are true thermodynamic phase transitions and hence that the GT and AT lines are *static* in nature, the time effects marking these transitions find no explanation whatsoever in terms of the MF models. Therefore, the next step is to ascertain whether or not the K-model [29, 33] offers some explanation for this finding. In the picture of an *infinite* three-dimensional (3D) ferromagnetic (FM) cluster (matrix) plus *finite* FM spin clusters (i.e., the K-model), finite spin clusters *coexist* with an infinite FM matrix at all temperatures below T_C (the Curie point) and interact [30] not only with one another but also with the FM matrix through *weak* long-range Ruderman–Kittel–Kasuya–Yosida (RKKY) interactions. As the temperature is lowered below T_C, spin clusters begin to *freeze* but the freezing process is not cooperative in the sense that not all of the clusters freeze in random orientations at the same temperature; freezing occurs over a wide range of temperatures [32] because of the distribution in cluster size and hence in cluster relaxation times. Alternatively, freezing is a *gradual* thermal blocking [2, 36, 46] process in which the cluster *largest* in size, due to its *slowest* relaxation rate, *appears* to be

frozen on the experimental timescale at the *highest* temperature (which lies below T_C) while, on the same timescale, the clusters of *smaller* size appear to freeze at *lower* temperatures as their relaxation rate progressively slows down with decreasing temperature (i.e., the so-called re-entrant mixed phase 1, denoted in figure 6 by RE(M_1^*), is formed in which an infinite FM matrix coexists with large, randomly oriented but 'frozen', clusters). As this type of thermal blocking process progresses, a temperature T^{**} is reached at which even the smallest cluster appears to be frozen. At this temperature, the spin system finds itself in a state (the re-entrant mixed phase 2, (RE(M_2^*)) in figure 6) in which finite FM spin clusters, frozen in random orientations, *coexist* with the infinite FM spin cluster. Consequently, in consonance with our recent FMR results [33], random anisotropy picks up in strength very rapidly as T is lowered below T^{**}. Moreover, the coercivity, which possessed a small value at temperatures in the range $T^{**} \lesssim T \lesssim T_C$, increases steeply for $T < T^{**}$ as a result of the pinning of domain walls (of the FM domains constituting the infinite FM matrix) at the boundaries of the frozen clusters embedded in the FM matrix. In conformity with this prediction, the coercivity (H_C) in the amorphous alloys in question [10, 15, 31, 35] is $\approx$0.1 Oe for temperatures close to T_C but increases slowly to $\approx$1 Oe as the temperature is lowered to a certain value (T^{**}) below which H_C increases *exponentially*, reaching values at 4.2 K that are *two to three orders of magnitude larger* than those at $T \simeq T_C$; T^{**} assumes *lower (higher)* values with increasing TM (Fe) concentration. As shown below, the above remarks have a direct bearing on the observed behaviour of 'field-cooled' (FC) and 'zero-field-cooled' (ZFC) magnetizations.

In the FC mode of measurement, the sample is cooled in *finite* external magnetic fields (H) from temperatures close to T_C where spin clusters as well as FM matrix spins are relaxing freely. Thus, at such temperatures even a *weak* field suffices to orient them towards its own direction and the cluster plus FM matrix spins get 'locked' into the field direction as the thermal-misaligning (disordering) tendency is progressively curtailed by the reduction in temperature. Consequently, regardless of the rate at which the sample is cooled, M_{FC} eventually attains a value close to that dictated by the demagnetizing factor and stays constant at that value down to the lowest temperature. Therefore, the cooling rate and anisotropies other than the shape anisotropy (e.g., the dipolar anisotropy or local random anisotropy brought into play by the clusters frozen in random orientations at low temperatures) have little or even no influence on $M_{FC}(T)$. On the other hand, in the ZFC mode of measurement, the field is stepped up from zero to a certain fixed value (H_f) at the lowest temperature T_l after the sample had been cooled to T_l in zero field. Sizable anisotropy at $T = T_l$ curbs the spin-ordering tendency of the external field, particularly at low fields ($H_f < 50$ Oe), so much so that H_f is unable to generate as much response (M_{ZFC}) as is expected when the countering action of the anisotropy is missing. As the temperature is raised, individual spins as well as the smallest clusters at temperatures just above T_l and larger clusters at higher temperatures are *set free* by thermal energy, because the height of the energy barrier for thermal activation increases with cluster size. Alternatively, at any given temperature, the cluster of smallest size has the fastest relaxation rate, since its thermal activation energy (E_a) is the lowest. With increasing temperature, increasing numbers of spin clusters are set free by thermal energy and the anisotropy diminishes rapidly, particularly at low temperatures, primarily due to the relaxation of small clusters. The external field is now more effective in ordering individual FM matrix spins and spin clusters, especially at low temperatures when the thermal energy is small, and M_{ZFC}, after growing initially at a very steep rate, tends to saturate at higher temperatures (an inference in agreement with the present observations; see figures 1 and 2). However, the duration of time for which the sample is kept at a temperature (i.e., the so-called 'waiting time',

t_W) or the heating rate plays a decisive role in determining M_{ZFC} (and hence the state of the spin system) at different temperatures, as elucidated below. If t_W is *reduced* or the sample is heated at a *faster* rate, the *effective* height of the activation barriers increases, the relaxation rate of all of the clusters *slows down* but the reduction in relaxation rate is *more significant* for *bigger* clusters than for smaller ones (this is so because E_a is already large for big clusters and even a small increment in E_a considerably slows down the relaxation rate) and anisotropy persists to higher temperatures and limits $M_{ZFC}(T)$ to *lower* values (the reduction in M_{ZFC} at a given temperature depends on the strength of the anisotropy at that temperature). Consequently, the $M_{ZFC}(T)$ curve starts coinciding with the $M_{FC}(T)$ curve at a much higher temperature. Thus, this mechanism accounts not only for the extreme (reduced) sensitivity of $T_{GT}(H) \equiv T_1(H)$ to the thermal cycling rate, TCR, at low (higher) fields but also for the relatively small or even zero shift in $T_{AT}(H) \equiv T_2(H)$ caused by the alteration of TCR. Moreover, the onset of weak irreversibility at T_{GT} and the crossover from weak to strong irreversibility at T_{AT} are attributed, in the K-model, to the appearance of *weak* 'frozen-in' random anisotropy (FRA) at $T \simeq T_{GT}$ and to a steep increase in the strength of the FRA for temperatures below T^{**} ($\simeq T_{AT}$), respectively, such that the Zeeman energy greatly exceeds the anisotropy energy at T_{GT} whereas the reverse is true at T_{AT}. This interpretation, in a sense, has a *parallel* in the results of the model for a Heisenberg spin glass (SG) with weak random anisotropy, proposed by Kotliar and Sompolinsky [25] (see section 2 for details), in which the finite-field transitions for this SG system in the limits of *weak* ($d \ll h^{5/2}$) and *strong* ($h^{2/3} \ll d$) anisotropy are of the GT and AT types, respectively.

As already stated above, weak (strong) FRA, in the K-model, originates from big (small) spin clusters frozen in random orientations at $T \simeq T_{GT}$ ($T \simeq T_{AT}$). It is, therefore, not surprising that the *average* cluster moment participating in the 'transition' at T_{GT} is *substantially larger* than that involved in the transition at T_{AT}, i.e., $\bar{\mu}_{GT} \gg \bar{\mu}_{AT}$. Progressive substitution of Co or Ni for Fe in a-$Fe_{90-x}TM_xZr_{10}$ (TM = Ni, Co) alloys results in the breaking up of finite spin clusters into smaller ones and the merging of some of them with the infinite FM matrix (for details, see [31]). Hence, as x increases, the number of spins within the infinite FM matrix increases at the expense of those forming the finite clusters, finite clusters shrink in size and decrease in number, the cluster size distribution narrows down and the average cluster size decreases. This prediction of the K-model also conforms well with the present observation that both $\bar{\mu}_{GT}$ and $\bar{\mu}_{AT}$ assume smaller values with increasing Co or Ni concentration (see the inset of figure 4). From the physical picture depicted above, we conclude that

(i) unlike the mean-field models [4, 5, 18, 24–26], the K-model [29–32] provides a satisfactory but qualitative explanation for the observed time-dependent effects associated with the GT and AT lines and thereby asserts that the GT and AT transitions are not the true thermodynamic phase transitions in the sense that not all of the *transverse* and *longitudinal* spin components cooperatively freeze at T_{GT} and T_{AT}, respectively, and

(ii) the GT and AT transitions are basically driven by 'frozen-in' random anisotropy brought about by the freezing of spin clusters with lowering temperature.

Finally, certain issues concerning the observed irreversibility lines in the H–T plane for the systems investigated here deserve serious consideration. For want of an appropriate nomenclature, the weak-irreversibility line and the weak-to-strong-irreversibility crossover line have been referred to as the 'GT' and 'AT' lines, respectively, in this paper. In sharp contrast with the mean-field GT and AT irreversibility lines, which are *static* and hence critical lines in the H–T phase diagram, the irreversibility lines in question are *dynamic* in nature and correspond to a certain observation time [46]. The result that $T_{GT}(H)$ and $T_{AT}(H)$

are TCR independent, so long as TCR $\lesssim 0.02$ K min^{-1} or the static mode of measurement is used, is a consequence of the limited resolution of the VSM and extremely slow (logarithmic) nature of the dynamics of re-entrant spin systems. It is with this perspective that the curves depicting the concentration dependences of $T_{GT}(0)$ and $T_{AT}(0)$ in figure 6 must be viewed. The results of the present investigation assert that time-dependent effects are an intrinsic property of the irreversibility lines but do not permit one to draw any definite conclusion about the exact nature of the dynamics. A direct approach that can be used to accomplish this is to determine these lines at different observation times (or frequencies) from ac susceptibility measurements taken in the presence of dc magnetic fields. Such a study is planned for the future.

5. Summary

Extensive bulk magnetization measurements have been performed on amorphous (a-) $Fe_{90-x}TM_xZr_{10}$ (TM = Co, Ni) and $Fe_{90+y}Zr_{10-y}$ re-entrant ferromagnetic alloys in both the static and the dynamic thermal cycling modes with a view to studying in detail the irreversibilities in low-field magnetization usually associated with the transition to the re-entrant state. The results of such investigations expose the inadequacies of the mean-field theories proposed in the literature for re-entrant ferromagnetic systems and clearly demonstrate that, contrary to popular belief, the transition to the re-entrant state in three-dimensional (3D) random quench-disordered spin systems with concentration just above the percolation threshold for long-range ferromagnetic order is not a true thermodynamic phase transition and the re-entrant state is not a pure spin-glass state but a *mixed* one in which ferromagnetic order coexists with *cluster* spin-glass order. All of the diverse aspects of the present results, i.e., the existence of Gabay–Toulouse (GT) and de Almeida–Thouless (AT) types of irreversibility line in the H–T plane as well as the time-dependent features of these lines, find qualitative but straightforward interpretation in terms of the picture of a 3D infinite ferromagnetic (FM) matrix plus finite FM spin clusters (i.e., the so-called K-model).

References

[1] Fischer K H and Hertz J A 1991 *Spin Glasses* (Cambridge: Cambridge University Press)
[2] Mydosh J A 1993 *Spin Glasses: an Experimental Introduction* (London: Taylor and Francis)
[3] Kaul S N 1995 *Met. Mater. Processes* **7** 29 and references cited therein
[4] de Almeida J R L and Thouless D J 1978 *J. Phys. A: Math. Gen.* **11** 983
[5] Gabay M and Toulouse G 1981 *Phys. Rev. Lett.* **47** 201
[6] Yeshurun Y, Salamon M B, Rao K V and Chen H S 1981 *Phys. Rev.* B **24** 1536
Geohegan J A and Bhagat S M 1981 *J. Magn. Magn. Mater.* **25** 17
[7] Beckman O, Figueroa E, Gramm K, Lundgren L, Rao K V and Chen H S 1982 *Phys. Scr.* **25** 726
Maletta H, Aeppli G and Shapiro S M 1982 *Phys. Rev. Lett.* **21** 1490
[8] Manheimer M A, Bhagat S M and Chen H S 1983 *J. Magn. Magn. Mater.* **38** 147
[9] Jonason K, Mattsson J and Nordblad P 1996 *Phys. Rev.* B **53** 6507
Jonason K, Mattsson J and Nordblad P 1996 *Phys. Rev. Lett.* **77** 2562
[10] Beck W and Kronmüller H 1985 *Phys. Status Solidi* b **132** 449
[11] Read D A, Moyo T and Hallam G C 1984 *J. Magn. Magn. Mater.* **44** 279
Read D A, Moyo T and Hallam G C 1986 *J. Magn. Magn. Mater.* **54–57** 309
[12] Lauer J and Keune W 1982 *Phys. Rev. Lett.* **48** 1850
Varret F, Hamzic A and Campbell I A 1982 *Phys. Rev.* B **26** 5285
[13] Manns V, Brand R A, Keune W and Marx R 1983 *Solid State Commun.* **48** 811
Abd-Elmeguid M M, Micklitz H, Brand R A and Keune W 1986 *Phys. Rev.* B **33** 7833
[14] Ghafari M, Gonser U, Wagner H G and Naka M 1982 *Nucl. Instrum. Methods* **199** 197
Ghafari M, Keune W, Brand R A, Day R K and Dunlop J B 1988 *Mater. Sci. Eng.* **99** 65

Ghafari M, Chmielek N, Keune W and Foley C P 1989 *Physica* B **161** 222
[15] Ryan D H, Coey J M D, Batalla E, Altounian Z and Ström-Olsen J O 1987 *Phys. Rev.* B **35** 8630
Ryan D H, Ström-Olsen J O, Provencher R and Townsend M 1988 *J. Appl. Phys.* **64** 5787
Ryan D H and Ren H 1991 *J. Appl. Phys.* **69** 5057
Ren H and Ryan D H 1995 *Phys. Rev.* B **51** 15 885
[16] Kunkel H P and Williams G 1988 *J. Magn. Magn. Mater.* **75** 98
[17] Mangin Ph, Boumazouza D, George B, Rhyne J J and Erwin R W 1989 *Phys. Rev.* B **40** 11 123
[18] Dubiel S M, Fischer K H, Sauer Ch and Zinn W 1987 *Phys. Rev.* B **36** 360
[19] Chamberlin R V, Hardiman M, Turkevich L A and Orbach R 1982 *Phys. Rev.* B **25** 6720
Malozemoff A P, Barnes S E and Barbara B 1983 *Phys. Rev. Lett.* **51** 1704
[20] Palumbo A C, Parks R D and Yeshurun Y 1983 *J. Magn. Magn. Mater.* **36** 66
Takzei G A, Kostyshin A M and Grebenyuk Yu P 1984 *Sov. Phys.–Solid State* **26** 1648
[21] Paulsen C, Hamida J A, Williamson S J and Maletta H 1984 *J. Appl. Phys.* **55** 1652
Taniguchi T and Miyako Y 1988 *J. Phys. Soc. Japan* **57** 3520
[22] Kenning G G, Chu D and Orbach R 1991 *Phys. Rev. Lett.* **66** 2923
Bernardot F and Rigaux C 1997 *Phys. Rev.* B **56** 2328
[23] Kunkel H, Roshko R M, Ruan W and Williams G 1991 *J. Appl. Phys.* **69** 5060
[24] Sherrington D and Kirkpatrick S 1975 *Phys. Rev. Lett.* **35** 1792
Kirkpatrick S and Sherrington D 1978 *Phys. Rev.* B **17** 4384
[25] Kotliar G and Sompolinsky H 1984 *Phys. Rev. Lett.* **53** 1751
[26] Fisher K H 1985 *Z. Phys.* B **60** 151
[27] Edwards S F and Anderson P W 1975 *J. Phys. F: Met. Phys.* **5** 965
[28] Coles B R, Sarkissian B V B and Taylor R H 1978 *Phil. Mag.* B **37** 489
[29] Kaul S N 1980 *Solid State Commun.* **36** 279
Kaul S N 1984 *IEEE Trans. Magn.* **20** 1290
Kaul S N 1985 *J. Magn. Magn. Mater.* **53** 5
[30] Kaul S N 1991 *J. Phys.: Condens. Matter* **3** 4027
Kaul S N 1988 *J. Phys. F: Met. Phys.* **18** 2089
[31] Kaul S N and Babu P D 1998 *J. Phys.: Condens. Matter* **10** 1563
[32] Kaul S N, Siruguri V and Chandra G 1992 *Phys. Rev.* B **45** 12 343
[33] Siruguri V and Kaul S N 1996 *J. Phys.: Condens. Matter.* **8** 4545
Siruguri V and Kaul S N 1996 *J. Phys.: Condens. Matter.* **8** 4567
[34] Babu P D and Kaul S N 1997 *J. Phys.: Condens. Matter.* **9** 7189
[35] Kaul S N 1983 *Phys. Rev.* B **27** 6923
Hiroyoshi H and Fukamichi K 1982 *J. Appl. Phys.* **53** 2226
[36] Kiss L F, Kemény T, Vincze I and Gránásy L 1994 *J. Magn. Magn. Mater.* **135** 161
[37] Kaptás D, Kemény T, Kiss L F, Balogh J, Gránásy L and Vincze I 1992 *Phys. Rev.* B **46** 6600
[38] Kaul S N, Bansal C, Kumaran T and Havalgi M 1988 *Phys. Rev.* B **38** 9248
[39] Michel R P and Weissman M B 1993 *Phys. Rev.* B **47** 574
Michel R P and Weissman M B 1994 *Phys. Rev.* B **50** 15 796
[40] Rhyne J J, Erwin R W, Fernandez-Baca J A and Fish G E 1988 *J. Appl. Phys.* **63** 4080
Mergia K, Messoloras S, Nikolaides G, Niarchos D and Stewart R J 1994 *J. Appl. Phys.* **76** 6380
[41] Fernández Barquin L, Gómez Sal J C, Kaul S N, Barandiarán J M, Gorria P, Pedersen J S and Heenan R 1996 *J. Appl. Phys.* **79** 5146
[42] Senoussi S, Hadjoudj S, Jouret P, Bilotte J and Fourmeaux R 1988 *J. Appl. Phys.* **63** 4086
Hadjoudj S, Senoussi S and Ryan D H 1990 *J. Appl. Phys.* **67** 5958
[43] Forkl A, Reisser R and Kronmüller H 1987 *Proc. Symp. on Magnetic Properties of Amorphous Metals* ed A Hernando, V Madurga, M C Sanchez-Trujillo and M Vazquez (Amsterdam: North-Holland) p 344
[44] Mirebeau I, Itoh S, Mitsuda S, Watanabe F, Endoh Y, Hennion M and Calmettes P 1990 *Phys. Rev.* B **41** 11 405
Mirebeau I, Itoh S, Mitsuda S, Watanabe F, Endoh Y, Hennion M and Calmettes P 1991 *Phys. Rev.* B **44** 5120
[45] Fernandez-Baca J A, Lynn J W, Rhyne J J and Fish G E 1988 *J. Appl. Phys.* **63** 3749
[46] According to the thermal blocking picture, the narrower the time window of the experimental probe, the higher the temperature at which the onset of the freezing process should be observed; such an observation has indeed been made previously [3, 32, 33] for the alloys under consideration.